Applied Physics Letters

RESEARCH ARTICLE | MARCH 30 2026

Optimal contact design for joule-heated systems

C. Cremers ; C. Wan ; J. A. Fan

Appl. Phys. Lett. 128, 134103 (2026)
https://doi.org/10.1063/5.0313180

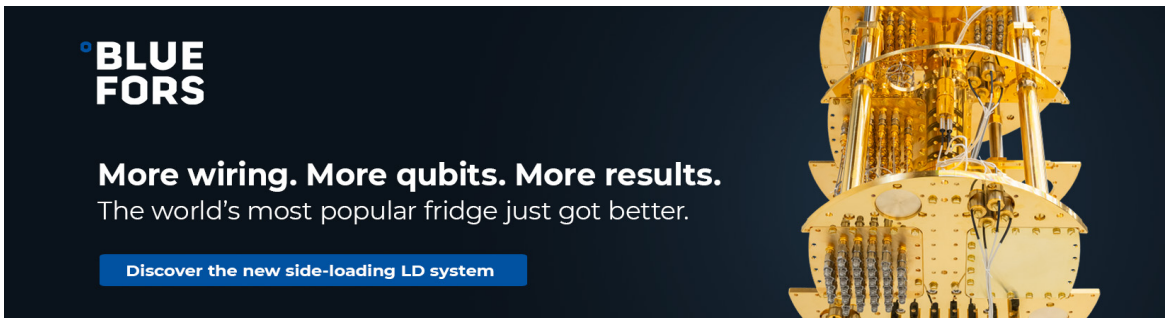

AIP Publishing

Applied Physics Letters ARTICLE pubs.aip.org/aip/apl

Optimal contact design for joule-heated systems

Cite as: Appl. Phys. Lett. **128**, 134103 (2026); doi: 10.1063/5.0313180
Submitted: 20 November 2025 · Accepted: 17 March 2026 ·
Published Online: 30 March 2026

C. Cremers, C. Wan, and J. A. Fan[a)]

AFFILIATIONS

Department of Electrical Engineering, Stanford University, Stanford, California 94305, USA

[a)]Author to whom correspondence should be addressed: jonfan@stanford.edu

ABSTRACT

Joule heating provides a straightforward and controllable method to convert electricity to heat at a resistive load, and it is used in a wide range of industrial and household systems. While the dissipation of electricity to heat is known to be highly efficient, heat losses at the electrical connection between the heating element and power supply can be significant, especially when considering that effective electrical conductors generally exhibit high thermal conductivities. Here, we present a straightforward derivation, using the Wiedemann–Franz law, to specify optimal designs for contacts in a manner that minimizes heat loss. We quantify the performance of these contacts for systems operating at different temperatures and scales and find that resistively heated microscale systems yield significant heat losses at contacts, and these losses dramatically decrease with increases in system scale. These results offer general guidelines to proper electrical contact design and present a more comprehensive picture of total energy efficiency in resistively heated systems.

Elevated temperatures are critical for many industrial and domestic applications, ranging from crystal growth and chemical synthesis to food preparation. For many systems, electrified heating approaches are utilized (Fig. 1), as they present a simple, modular, and highly controlled approach to heating and also enable the production of heat in a sustainable manner when green electricity is used. The most straightforward and widely used way to produce heat via electrification is joule heating, in which current passes through a resistive element and dissipates as heat.[1] Joule heating converts all electrical energy into heat, and it generally features minor parasitic losses in the power electronics.[2]

Fully understanding the loss mechanisms in joule-heated systems is critical, particularly in industrial scale systems that consume enormous amounts of power. One commonly cited consideration when using joule heating to produce high grade heat is the management of parasitic power loss at the electrical contacts to the heating element.[2,3] Power loss arises due to resistive heating in the contact itself and heat extraction arising from temperature gradients along the contact. To minimize these losses, contacts would ideally feature high thermal resistance and low electrical resistance. However, typical materials with high thermal resistance also have high electrical resistance, presenting a critical engineering challenge around managing both joule and thermal loss mechanisms in contacts.

In this study, we investigate the role of contacts in joule-heated systems using the Wiedemann–Franz law (WFL), which couples electrical and thermal conductivity by accounting for the fact that electrons carry both current and heat in good conductors. The WFL specifically states that $\sigma = \kappa/LT$, where σ is the electrical conductivity, κ is the thermal conductivity, L is a constant known as the Lorenz number, and T is the temperature.[4] In ideal metals, L takes the Sommerfeld value of $2.44 \times 10^{-8}\ \mathrm{V^2/K^2}$. The application of the WFL to heating of contacts was first studied by Kohlrausch, who rigorously showed that the electrical potential at any point between two electrodes relates to its temperature relative to the electrodes and the Lorenz number of the material.[5] These results have been utilized to study the electro-thermal performance of high power electrical plug designs,[6–8] to understand the formation and behavior of contact spots at metal–metal interfaces,[9,10] and to determine the Lorenz numbers for metals.[11] In this study, we perform a simplified version of Kohlrausch's analysis to evaluate heat flow in systems where one of the electrodes is held at an elevated temperature by design. We specifically design contacts that optimally balance the need for high electrical conductivity with the need for minimal thermal conductivity, and we quantify energy losses from optimal contacts in systems ranging from microscale to industrial scale sizes, which has particular pertinence in electrified thermochemical reactor performance.

As in Kohlrausch's work, we will assume the ends of our contact are at given reservoir temperatures and there is no heat loss from the contact to the environment other than through the reservoirs. We will further specify a contact geometry consisting of an extruded metallic material with a constant cross-sectional area resulting in currents and temperatures being uniform in the cross section, but as per Kohlrausch's work, our results extend to arbitrary geometries. In our

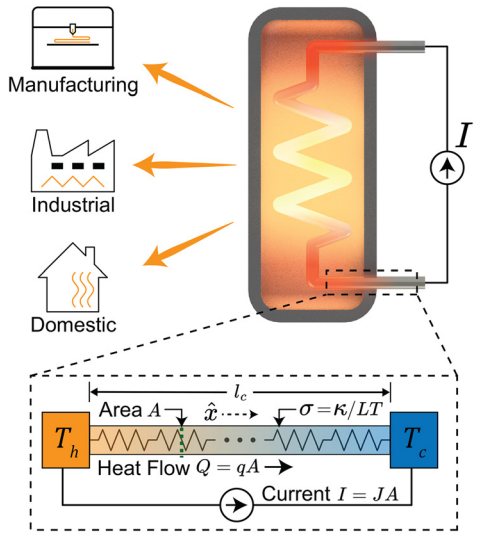

FIG. 1. Electrical contact model for a joule-heated system. Model of a generic joule-heated system consisting of a heated element connected to a power supply. This configuration generally describes various applications, including resistively heated chemical reactors, toasters, and 3D printer hotends. We model the contact as a distributed thermal resistance between a cold reservoir (temperature T_c) and a hot reservoir (temperature T_h) where a fixed electrical current I flows through the system. The contact has a length l_c and cross-sectional area A, and its electrical and thermal conductivities are σ and κ, respectively, which relate by the Wiedemann–Franz law. Parasitic heat losses are represented by the heat flux Q flowing to the cold reservoir.

electrical model, the current $I = J_x A$ is carried by the distributed conductance per unit length of $\Sigma = \sigma A$ of the contact, where A is the cross-sectional area of the contact.

For the thermal model, the power electronics supplying current into our system have a maximum operating temperature typically between 50 and 100 °C. Excess heat must be extracted to enforce temperature regulation, hence representing a cold reservoir. It is also possible the cold reservoir is specified upstream of the power electronics due to material compliance or safety requirement considerations in the system. The elevated operating temperature of the resistive device acts as a hot reservoir. These reservoirs are connected by contacts described with a distributed thermal conductivity per unit length of $K = \kappa A$, related to the electrical conductivity via the WFL $\Sigma = K/LT$, and heat flow at any point of the contact is $Q = qA$, where q is heat flux. The heat transferred into the cold reservoir Q_c is wasted energy, and it is extracted using a heat sink or heat exchanger to maintain the temperature of the cold reservoir.

To find the optimal conductivity condition in which system losses at contacts are minimized, we write the heat equation in its most general form

$$\rho c_p \frac{\partial T}{\partial t} - \nabla \cdot (\kappa \nabla T) = \dot{q}_v, \tag{1}$$

where ρ is the material density, c_p is the heat capacity at constant pressure, T is the temperature, t is time, and $\dot{q}_v = |\vec{J}|^2/\sigma$ is the volumetric heat dissipation from resistive losses. As most industrial systems operate continuously, our system is in a steady state, and hence we drop the time derivative term $\partial T/\partial t$. Furthermore, as our contact cross section has uniform current density and temperature, we may neglect derivatives in T and κ in the direction normal to the contact, here $\hat{x}$. With these simplifications, the heat equation reduces to the form $0 = \partial_x \cdot (\kappa \partial_x T) + J_x^2/\sigma$. Finally, we can multiply by the cross-sectional area to derive

$$0 = \frac{I^2}{\Sigma} + \frac{d}{dx}\left(K\frac{dT}{dx}\right), \tag{2}$$

$$= \frac{I^2}{\Sigma} - \frac{dQ}{dx}. \tag{3}$$

In these expressions, thermal gradients are specified along the contact (i.e., the x direction) and heat generation due to joule heating within the contact is I^2/Σ. Simplifications are achieved using the definition of heat flow along the contact, $Q = -K \times dT/dx$. In general, Q explicitly depends on temperature, $T(x)$, and we apply the chain rule to find $dQ/dx = \partial Q/\partial T \times \partial T/\partial x$. With this and application of the WFL, we find

$$\frac{LTI^2}{K} = \frac{\partial Q}{\partial T}\frac{\partial T}{\partial x} \rightarrow LTI^2 = -Q\frac{\partial Q}{\partial T}. \tag{4}$$

We experimentally validate our problem formulation (see supplementary material S1), and we identify the solution to Eq. (4),

$$|Q(T)| = I\sqrt{L}\sqrt{T_m^2 - T^2}. \tag{5}$$

The absolute value for Q is necessary as both signs of Q solve Eq. (4). T_m is a constant, and its value generally depends on contact design; see more in supplementary material S2. Mathematically, T_m must be greater than or equal to T_h, otherwise Q is imaginary and nonphysical.

As Q may take either sign, heat may flow in either direction in the contact. We thus identify two scenarios for our contact design. In one, Q does take both signs, and heat does flow toward both the hot and cold reservoirs. We interpret this as excess heat generation within the contact resulting in a hot spot with temperature $T_m > T_h$, as observed in the bottom panel of Fig. 2(a). Heat flows from the contact hot spot into both the cold and hot reservoirs, which is represented by the zero crossing of the heat flow shown in the top panel of Fig. 2(a). Here, the electrical conductance of the contact is too low, or alternatively, the aspect ratio of the contact l_c/A is too high given the conductivity of the selected material. In the other scenario, Q always takes the same sign, meaning heat is extracted from the hot reservoir and flows to the cold reservoir along with any dissipation in the contact. This implies the temperature monotonically decreases from T_h to T_c. While no part of the contact reaches T_m, which no longer has a clear physical interpretation, the temperature and heat flow profile is identical to the $T < T_h$ region of a low conductance contact with maximum temperature T_m. In this case, the electrical conductivity of the contact is too high, i.e., the aspect ratio of the contact l_c/A is too low given the conductivity of the selected material.

The ideal operating condition for contact design that minimizes energy loss is the critical point separating these scenarios, which occurs when $T_m = T_h$. This condition minimizes the heat rejection to the cold reservoir. Furthermore, $Q(T_h) = 0$ at this point, such that no heat is exchanged with the hot reservoir, and heat generation in the contact perfectly balances the extraction. This condition makes

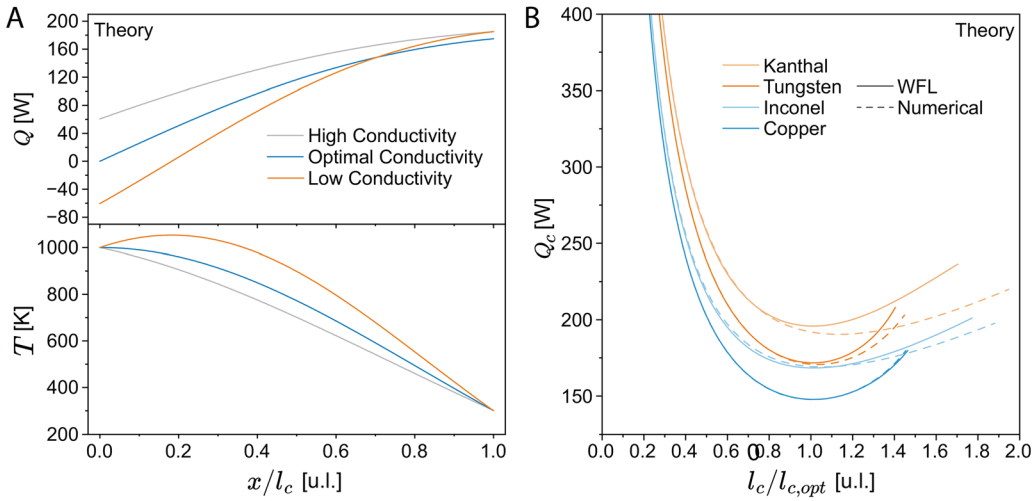

FIG. 2. Theoretical models of contact heat loss. (a) Heat flow (top) and temperature (bottom) profiles along three tungsten contacts with differing lengths, using the room temperature Lorenz number for tungsten. (b) Plots of total heat loss through various contacts as a function of normalized contact length, assuming an electrical current drive of 1000 amps and hot and cold reservoir temperatures of 1000 and 300 K, respectively, for each contact. Different contact metals and lengths are considered, and the curves are calculated using an ideal WFL description of the contact material (solid lines) and with empirical, temperature dependent electrical and thermal conductivities (dashed lines).

physical sense: if heat is flowing into the hot reservoir, the hottest point of the contact effectively serves as a new hot reservoir with a temperature greater than T_h. If heat is leaving the hot reservoir, one could simply increase the resistivity, decreasing heat extraction. Importantly, as in Kohlrausch's work, our model presents general results that show optimal heat loss through contacts depends solely on material Lorenz number, operating temperature, and required current. A long contact from copper or a short contact from nickel-chrome superalloys will have similar heat extraction, up to the difference in Lorenz numbers, if sized appropriately. Furthermore, cylindrical, rectangular, or even nonuniform contact cross sections will exhibit identical heat extraction when optimized.

To derive optimal contact geometries that minimize losses for a given resistively heated system, we evaluate Eq. (5) at our ideal operating condition. Together with Ohm's law, the resistance of our ideal contact is determined to be $R_{opt} = \sqrt{L}\sqrt{T_h^2 - T_c^2}/I$, which is consistent with Kohlrausch's result. With arbitrary $\kappa(T)$, closed form relationships describing contact design are not possible, and the optimal ratio between contact length and cross section must be evaluated by the following numerical integration:

$$\frac{l_{c,opt}}{A} = \frac{1}{I\sqrt{L}} \int_{T_c}^{T_h} \frac{\kappa(T)}{\sqrt{T_h^2 - T^2}} dT. \tag{6}$$

This expression accounts for the temperature dependence of the electrical and thermal conductivities of the contact material. For contacts featuring a nonuniform cross-sectional area, we can use an expression for the average cross-sectional area in our solution, $A_{avg} = \int_0^{l_c} A dx/l_c$, as long as the axial variation in A is smooth enough for the current distribution in the contact to be approximately uniform. More complex geometries may require finite element analysis models or methods like those described by Greenswood and Williamson.[12]

Our analysis can extend to scenarios where contact material behavior deviates from the WFL. In these situations, our optimal contact condition (i.e., $T_m = T_h \rightarrow Q(T_h) = 0$) still holds, and we can numerically integrate Eq. (2) using empirical values for the electrical and thermal conductivities until the cold reservoir temperature is reached to find l_c. The temperature gradient can be readily evaluated to quantify heat loss from the contacts.

To evaluate the properties of various contact configurations, we plot heat loss as a function of contact length for several candidate metals described using both the ideal WFL and by integrating Eq. (2) with appropriate material properties.[13–18] For the WFL analyses, we integrate $\kappa(T)$ and use experimental values of the Lorenz numbers at the average of the cold and hot reservoir temperatures. The results are shown in Fig. 2(b), where contact length has been normalized to the optimal contact length $l_{c,opt}$ as calculated with the WFL. We generally observe excellent agreement between the two models for all materials except for Kanthal, where limited availability of low temperature thermal conductivity data leads to discrepancies.

Critically, these plots indicate that having an insufficiently conductive contact can quickly lead to extreme temperatures and contact breakdown. As noted by Greenwood and Williamson,[12] contact failure is mitigated in materials like nickel-chrome superalloys and Kanthal, which have conductivities that increase with temperature.[17,18] In the opposite limit where the contact is excessively conductive, there is no catastrophic failure, but there is significant excessive power loss. As an example, a copper contact featuring a length that is 30% the optimal value will more than double the amount of heat extracted from the load. These observations indicate that in practice, the ideal experimental contact design should be slightly shorter than the theoretically optimal contact length, which would provide margin against material failure while only slightly increasing losses.

We next consider if the derived design rules result in practical structures. For example, consider a system operating at 1000 amps and 600 °C with a contact length of 0.25 m. Assuming that the contact consists of Inconel 625 with $\kappa \sim 15$ W/mK,[17] optimal contact conditions specify that the wire should have a 5.5 cm diameter. If we instead

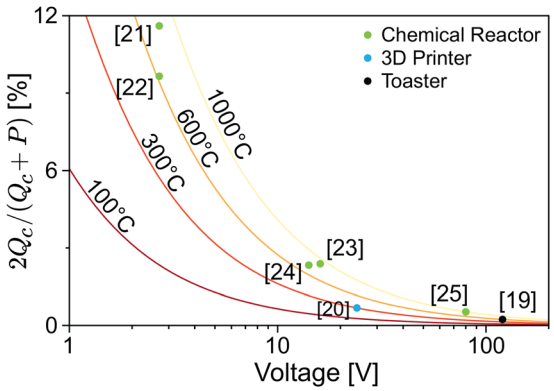

FIG. 3. Practical model outcomes assuming ideally designed contacts. A plot of the fraction of power lost to ideal contacts as a function of voltage for several temperatures, assuming a Lorenz number of 3×10^{-8} V^2/K^2. We evaluate the performance of household appliances like toasters,[19] manufacturing tools like 3D printers,[20] and industrial applications like emerging electrified chemical reactors.[21–25]

operate at 1000 °C with tungsten, which exhibits a $\kappa \approx 150$ W/mK,[13] optimal contact conditions specify that the wire has a 0.9 cm diameter wire. These values are practically achievable. Furthermore, as the ideal contact radius $r_c \propto \sqrt{l_c I}$, the contact dimensions will likely be reasonably achieved for a wide range of joule-heated system configurations and scales.

Using the results of the model, we compute the fraction of power lost to contacts in joule-heated systems, assuming optimal designs. For this analysis, we observe that the proportionality between heat loss and current delivery yields a heat loss per unit power delivered of $Q_c/P = \sqrt{L}\sqrt{T_h^2 - T_c^2}/\sqrt{RP} = \sqrt{L}\sqrt{T_h^2 - T_c^2}/V$ for each contact. As such, to minimize energy loss through contacts, we desire high power, high resistance loads that require large voltages to drive. We plot fractional system power loss to the contacts, $2Q_c/(2Q_c + P)$, as a function of voltage across the load for several temperatures in Fig. 3, which assumes the system comprises two contacts connected to the load.

An evaluation of ideal contact heat loss in the context of various industrial and household joule-heated systems is presented in the figure. A kitchen toaster powered by line voltage operating at 600 °C loses about 0.2% through its contacts.[19] A 3D printer extruder at 24 V and 300 °C has losses of around 0.7%.[20] For scaled joule-heated thermochemical reactors, systems that deliver around 15 kW at 80 V and that operate at 1000 °C yield ideal contact losses as little as 80 W, which constitutes just 0.5% of total input power.[25] However, for microscale thermochemical reactors comprising a joule-heated superalloy metal tube driven with a voltage of around 2.7 V, the high currents delivered would yield contact losses of 12.9 W, corresponding to a total power efficiency reduction of 12%.[21] We note that this analysis assumes ideal contacts, and suboptimal contacts will exhibit worse power efficiencies. In Ref. 21, the reported temperature gradients at the ends of the reactor suggest the presence of non-ideal short contacts, yielding a system power efficiency reduction of 18% due to contact losses.

This analysis has significant implications on viable configurations for joule-heated thermochemical systems, where the enormous energy requirements and low margins require systems to operate with near unity efficiency. For example, Balakotaiah and Ratnakar proposed various resistive networks that could be heated, including multitubular schemes, metallic monoliths, and parallel wires.[26] The parallel wire setup consisted of wires with diameters between 100 and 1000 μm, and a specific presented toy example involved 1 m long, 100 μm diameter wires powered by 41 V that reached temperatures as high as 1200 K. Based on our analysis, scaling up via the parallelization of microheating elements yields the same contact losses as a single microheating element, as each unit requires the same voltage. For the toy example, we calculate that 1% of the input power is lost through the contacts, independent of the number of parallel wires in the system. If we were to instead consider a more robust 0.5 m long, 1000 μm diameter wire, our voltage drops to 2 V and 16% of the power is lost through the contacts. In this scenario, the resistive network should be configured with the wires electrically in series rather than in parallel, which raises integration challenges.

Next, we discuss limitations of the model and the ways in which practical implementations might deviate from our calculations. While our requirement of having the resistive load at an elevated temperature and the power supply at a lower temperature validates the existence of a hot and cold reservoir, it is unrealistic to assume there is no heat loss to the environment along the contact. However, we observe that the presence of heat loss to the environment strictly serves to increase total heat loss via the contacts.

Our current model also is limited to DC loading. For a power electronics schemes utilizing AC power, skin effects can manifest and effectively increase the electrical resistance without affecting the thermal conductivity. This acts to increase the Lorenz number, thus increasing losses. We also note that some applications of joule heating involve intermittent loading, for example, running with some current I when abundant solar electricity is available and $I/2$ otherwise. This would aggravate our contact problem, as the contacts would extract excess power during the low utilization phase. For example, The microreactor in Ref. 21 would lose 26% of its input power when operated at half current.

Beyond the macroscopic limitations, we consider limitations of the WFL, which critically assumes that electrons carry both the electrical current and the heat in the material. The contribution to the thermal conductivity from phonons may break this assumption down to varying extents.[27] However, phonon contributions serve to increase the Lorenz number, which we wish to avoid. As such, we should generally stick with materials with negligible phonon contributions. As we saw in Fig. 2(b), using the WFL is sufficient for most metals.

Additionally, while the WFL has been well studied for bulk materials, interfaces are more complicated. Studies indicate that an interfacial form of the WFL holds for high quality interfaces between metals such as those produced via deposition.[28] However, in physically assembled contacts, significant heat can also be carried through the air gap between interface asperities.[29] This violates our model, as heat is exchanged through the environment outside the contact, but it may be accounted for with various methods described in supplementary material S4. Additionally, interfaces can make it challenging to properly design contacts due to their less predictable properties, which are generally a function of design, fabrication, and operation details.[9,30]

A design can outperform the model if the heat from the contact can be recovered and utilized. For example, in the application of a joule-heated reactor, the reactant gas could flow along the contact,

preheating the gas with the contact losses. However, such concepts present additional system level design challenges.

In summary, our application of the WFL to contacts presents a reasonable and straightforward bound on how efficient a joule-heated system can be without explicit design for heat recovery. We find that contact losses are relatively minimal in large scale systems with well designed resistive networks but that they can be significant in smaller devices such as joule-heated microreactors. Importantly, the usual goal of minimizing contact resistance is potentially detrimental in these systems, and instead heat extraction must be balanced with efficient current delivery. With the use of experimental Lorenz numbers, it should be achievable to design contacts with optimal heat loss properties.

See the supplementary material for the sections discussing the experimental validation of our results, solving the contact temperature profile, design considerations when utilizing multiple materials, and design considerations in the presence of interfaces. Additionally, code to solve the contact problem is available.

J.A.F. acknowledges support from the Department of Energy under Agreement No. DE-EE0011191, the Stanford School of Sustainability Accelerator under Agreement No. 266899, and EPIXC under Agreement No. M2505270. C.C. acknowledges support from the Stanford Graduate Fellowship.

AUTHOR DECLARATIONS

Conflict of Interest

The authors have no conflicts to disclose.

Author Contributions

C. Cremers: Conceptualization (equal); Data curation (equal); Formal analysis (equal); Methodology (equal); Software (equal); Validation (equal); Visualization (equal); Writing – original draft (equal); Writing – review & editing (equal). **C. Wan:** Conceptualization (supporting); Methodology (supporting); Visualization (supporting). **J. A. Fan:** Conceptualization (equal); Funding acquisition (equal); Project administration (equal); Supervision (equal); Writing – original draft (equal); Writing – review & editing (equal).

DATA AVAILABILITY

The data that support the findings of this study are available from the corresponding author upon reasonable request within the article and its supplementary material.

REFERENCES

[1]D. S. Mallapragada, Y. Dvorkin, M. A. Modestino, D. V. Esposito, W. A. Smith, B.-M. Hodge, M. P. Harold, V. M. Donnelly, A. Nuz, C. Bloomquist, K. Baker, L. C. Grabow, Y. Yan, N. N. Rajput, R. L. Hartman, E. J. Biddinger, E. S. Aydil, and A. D. Taylor, "Decarbonization of the chemical industry through electrification: Barriers and opportunities," Joule **7**, 23–41 (2023).

[2]L. Zheng, M. Ambrosetti, and E. Tronconi, "Joule-heated catalytic reactors toward decarbonization and process intensification: A review," ACS Eng. Au **4**, 4–21 (2024).

[3]L. Zheng, D. Wang, Y. Jiang, Y. Ren, Y. Wu, Y. Fu, and J. Zhang, "Volumetric internal joule heating of a catalyst packed sisic foam for efficient dry reforming of methane," Chem. Eng. J. **503**, 158291 (2025).

[4]R. Franz and G. Wiedemann, "Ueber die wärme-leitungsfähigkeit der metalle," Ann. Phys. **165**, 497–531 (1853).

[5]F. Kohlrausch, "Ueber den stationären temperaturzustand eines elektrisch geheizten leiters," Ann. Phys. **306**, 132–158 (1900).

[6]M. Gatzsche, N. Lücke, S. Großmann, T. Kufner, B. Hagen, and G. Freudiger, "Electric-thermal performance of contact elements in high power plug-in connections," in *2014 IEEE 60th Holm Conference on Electrical Contacts (Holm)* (IEEE, 2014), pp. 1–8.

[7]M. Gatzsche, N. Lücke, S. Großmann, T. Kufner, and G. Freudiger, "Validity of the voltage-temperature relation for contact elements in high power applications," in *2015 IEEE 61st Holm Conference on Electrical Contacts (Holm)* (IEEE, 2015), pp. 29–38.

[8]W. Ren, J. Wei, X. Meng, and H. Zhi, "Numerical simulation of temperature–voltage relation in electrical contacts and correction of classical Kohlrausch's equation," IEEE Trans. Electron Devices **63**, 1217–1224 (2016).

[9]S. Timsit, "Electrical contact resistance: Properties of stationary interfaces," in *Electrical Contacts - 1998. Proceedings of the Forty-Fourth IEEE Holm Conference on Electrical Contacts (Cat. No.98CB36238)* (IEEE, 1998), pp. 1–19.

[10]J. Williamson and N. Allen, "Thermal stability in graphite contacts," Wear **78**, 39–48 (1982).

[11]B. Hay, "A brief history of the thermal properties metrology," Measurement **155**, 107556 (2020).

[12]J. A. Greenwood and J. B. P. Williamson, "Electrical conduction in solids. ii. theory of temperature-dependent conductors," Proc. R. Soc. London, Ser. A **246**, 13–31 (1958).

[13]The Space Nuclear Propulsion Project Team, "St-23 space nuclear propulsion material property handbook," Report No. SNP-HDBK-0008 (National Aeronautics Space Administration, Marshall Space Flight Center, Alabama, 2024).

[14]F. Hu and S. Lucyszyn, "Emerging thermal infrared 'THz Torch' technology for low-cost security and defence applications," in *THz and Security Applications*, edited by C. Corsi and F. Sizov (Springer Netherlands, Dordrecht, 2014), pp. 239–275.

[15]C. Y. Ho, R. W. Powell, and P. E. Liley, "Thermal conductivity of the elements," J. Phys. Chem. Ref. Data **1**, 279–421 (1972).

[16]R. A. Matula, "Electrical resistivity of copper, gold, palladium, and silver," J. Phys. Chem. Ref. Data **8**, 1147–1298 (1979).

[17]S. Metals, *Inconel Alloy 625* (Special Metals, Battelle Memorial Institute, Ohio, 2025).

[18]Kanthal, *Kanthal A-1 Strip Datasheet* (Kanthal, 2024).

[19]M. Newborough, W. Batty, and S. Probert, "Design improvements for the ubiquitous electric toaster," Appl. Energy **27**, 1–52 (1987).

[20]Bambu Lab, *Bambu Lab A1 Mini 3D Printer* (Bambu Lab, 2025).

[21]S. T. Wismann, J. S. Engbaek, S. B. Vendelbo, F. B. Bendixen, W. L. Eriksen, K. Aasberg-Petersen, C. Frandsen, I. Chorkendorff, and P. M. Mortensen, "Electrified methane reforming: A compact approach to greener industrial hydrogen production," Science **364**, 756–759 (2019).

[22]Q. Dong, Y. Yao, S. Cheng, K. Alexopoulos, J. Gao, S. Srinivas, Y. Wang, Y. Pei, C. Zheng, A. H. Brozena, H. Zhao, X. Wang, H. E. Toraman, B. Yang, I. G. Kevrekidis, Y. Ju, D. G. Vlachos, D. Liu, and L. Hu, "Programmable heating and quenching for efficient thermochemical synthesis," Nature **605**, 470–476 (2022).

[23]L. Zheng, M. Ambrosetti, D. Marangoni, A. Beretta, G. Groppi, and E. Tronconi, "Electrified methane steam reforming on a washcoated SiSiC foam for low-carbon hydrogen production," AIChE J. **69**, e17620 (2023).

[24]E. B. Ledesma, M. Idamakanti, P. Bollini, M. P. Harold, and R. R. Ratnakar, "Decarbonizing steam-methane reforming: Enhancing activity through joule heating of a Ni/ZrO_2-coated fecral coil," ChemCatChem **16**, e202301110 (2024).

[25]T. N. From, B. Partoon, M. Rautenbach, M. Østberg, A. Bentien, K. Aasberg-Petersen, and P. M. Mortensen, "Electrified steam methane reforming of biogas for sustainable syngas manufacturing and next-generation of plant design: A pilot plant study," Chem. Eng. J. **479**, 147205 (2024).

[26]V. Balakotaiah and R. R. Ratnakar, "Modular reactors with electrical resistance heating for hydrocarbon cracking and other endothermic reactions," AIChE J. **68**, e17542 (2022).

[27]Y. Chen, J. Ma, and W. Li, "Understanding the thermal conductivity and Lorenz number in tungsten from first principles," Phys. Rev. B **99**, 020305 (2019).
[28]R. B. Wilson and D. G. Cahill, "Experimental validation of the interfacial form of the Wiedemann-Franz law," Phys. Rev. Lett. **108**, 255901 (2012).
[29]T. S. Wiśniewski, "Experimental study of contacting surfaces microgeometry and gas gap impact on thermal contact conductance of metallic joints," Int. J. Heat Mass Transfer **200**, 123511 (2023).
[30]P. Slade, *Electrical Contacts: Principles and Applications*, 2nd ed. (CRC Press, Florida, 2017).